Solution Conformation of Salmon Calcitonin in Sodium Dodecyl Sulfate Micelles As Determined by Two-Dimensional NMR and Distance Geometry Calculations

Andrea Motta,*,‡ Annalisa Pastore,§ Nagana A. Goud,‖ and Maria A. Castiglione Morelli§,⊥

Istituto per la Chimica di Molecole di Interesse Biologico del CNR, 80072 Arco Felice, Napoli, Italy, European Molecular Biology Laboratory, 6900 Heidelberg, Germany, and Bachem Incorporated, Torrance, California 90505

Received April 2, 1991; Revised Manuscript Received July 10, 1991

ABSTRACT: The 32 amino acid hormone salmon calcitonin was studied at pH 3.7 and 7.4 by two-dimensional NMR in sodium dodecyl sulfate (SDS) micelles at 310 K. The spectrum was fully assigned, and the secondary structure was obtained from nuclear Overhauser enhancement spectroscopy (NOESY), $^3J_{HN\alpha}$ coupling constants, and slowly exchanging amide data. Three-dimensional structures consistent with NMR data were generated by using distance geometry calculations. A set of 260 interproton distances, derived from NOESY, and hydrogen-bond constraints, obtained from analysis of the amide exchange, were used. From the initial random conformations, 13 distance geometry structures with minimal violations were selected for further refinement with restrained energy minimization. In SDS, at both pHs, the main conformational feature of the hormone is an α-helix from Thr^6 through Tyr^{22}, thus including the amphipathic 8–22 segment and two residues of the Cys^1–Cys^7 N-terminal loop. The C-terminal decapeptide forms a loop folded back toward the helix. The biological significance of this conformation is discussed.

Calcitonin (CT)[1] is a single polypeptide chain hormone synthesized and stored by the parafollicular cells of the thyroid, parathyroid, and thymus glands. CT seems to be involved in many biological functions; however, its main action, and certainly the one of major physiological importance, is inhibition of bone resorption of regulating both the number and activity of osteoclasts (Breimer et al., 1988). Several mammalian and submammalian calcitonins have been isolated, sequenced, and synthesized, displaying considerable differences in amino acid composition (Dayhoff, 1978). In its common form, it consists of 32 amino acids with an N-terminal disulfide bridge between positions 1 and 7 and a C-terminal proline amide residue. Only eight residues are common to all species so far studied, and these are clustered at the two ends of the molecule. Methods for predicting the secondary structure of proteins indicate that the central region is helical (Merle et al., 1979) with an amphipathic character. An amphipathic helix defines a general α-helix domain containing opposing polar and nonpolar "faces" (Segrest et al., 1990). This structure has been reported to be important for the interaction with lipids of polypeptide hormones of diverse sequence (Epand, 1983), including sCT (Epand et al., 1983).

CD (Epand et al., 1983) and NMR (our unpublished results) studies have indicated that calcitonins have a low content of secondary structure in aqueous solution but they become more helical in the presence of structure-promoting solvents. In fact, NMR studies on sCT in aqueous TFE (Meyer et al., 1991) and MeOH (Meadows et al., 1991) indicated that the core of the hormone between residues 8 and 22 assumes an α-helical structure. Also hCT has been shown to form an α-helix in TFE (Doi et al., 1989). We have recently reported that sCT (Motta et al., 1989) and hCT (Motta et al., 1991) in the so-called cryomixtures (Motta et al., 1987, 1988) assume an extended conformation with only short double-stranded antiparallel β-sheet regions and no evidence of a regular helical segment.

Scheme I: Amino Acid Sequence of sCT

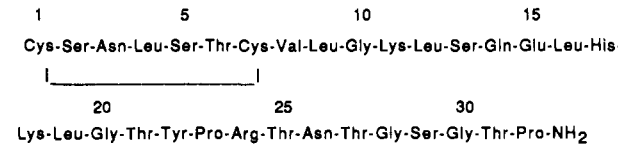

The CD mean-residue ellipticity values of several sCT–lipid complexes (Epand et al., 1983, 1986a), as well as of sCT–SDS (Epand et al., 1985), indicate the presence of about 50% helical content.

Accordingly, a membrane-like environment, such as that brought about by surfactant micelles, can be usefully applied to study the conformational properties of sCT at the interface and to simulate the catalytic role of membrane (Schwyzer, 1986). In this paper, we report on the conformation of sCT (Scheme I) in SDS micelles, as studied by ^{1}H NMR and distance geometry calculations.

‡ Istituto per la Chimica di Molecole di Interesse Biologico del CNR.
§ European Molecular Biology Laboratory.
‖ Bachem Inc.
⊥ Present address: Dipartimento di Chimica, Università della Basilicata, 85100 Potenza, Italy.

[1] Abbreviations: CT, calcitonin; sCT, salmon calcitonin; CD, circular dichroism; NMR, nuclear magnetic resonance; TFE, trifluoroethanol; MeOH, methanol; hCT, human calcitonin; SDS, SDS_{d25}, fully protonated and perdeuteriated sodium dodecyl sulfate; pH*, uncorrected glass-electrode reading; TSP, 3-(trimethylsilyl)propionic acid Na salt; 2D, two dimensional; DQF-COSY, two-dimensional double-quantum filtered correlated spectroscopy; NOESY, two-dimensional nuclear Overhauser enhancement spectroscopy; TOCSY, total correlation spectroscopy; $^3J_{HN\alpha}$, vicinal coupling constant between NH and α protons; 1D, one dimensional; NOE, nuclear Overhauser enhancement; $d_{\alpha N}(i,i+n)$, distance between the αCH of residue i and the NH of residue $i+n$; $^3J_{\alpha\beta}$, vicinal coupling constant between α and β protons; DG, distance geometry; EM, energy minimization; REM, restrained energy minimization; RMSD, root-mean-square difference; $d_{N\alpha}$, intraresidue distance between the αC H and the NH; $d_{\alpha N}$, distance between the αCH of residue i and the NH of residue $i+1$; d_{NN}, distance between the NH protons of residues i and $i+1$; $d_{\alpha\beta}(i,i+3)$, distance between the αCH of residue i and the β proton(s) of residue $i+3$.

0006-2960/91/0430-10444$02.50/0

Materials and Methods

NMR Experiments. sCT was prepared at Bachem Inc., Torrance, CA, and SDS_{d25} was purchased from Cambridge Isotope Laboratories (Woburn, MA).

For the acquisition of NMR spectra, 5×10^{-3} M of sCT in 95% ^1H_2O/5% ^2H_2O (at pH 3.7 and 7.4) or in 100% ^2H_2O (at pH* 3.3 and 7.0) were used. Isotopically labeled solvents originated from Aldrich (Milwaukee, WI). A solution of SDS_{d25} was added to a solution of the hormone, and the final mixture remained transparent. The concentration of SDS_{d25} was maintained well above the critical micelle concentration, with a final sCT–SDS_{d25} ratio of 1:180.

^1H spectra were recorded at 400 and 500 MHz with Bruker AM-400 and AM-500 spectrometers, both interfaced to an Aspect 3000 computer, at 310 K, and referenced to internal TSP.

2D experiments, namely, phase-sensitive DQF-COSY (Piantini et al., 1982), NOESY (Macura & Ernst, 1980), and TOCSY (Braunschweiler & Ernst, 1983; Bax & Davis, 1985), were run according to the time-proportional phase incrementation scheme (Drobny et al., 1979). Usually 512 equally spaced evolution time period t_1 values were acquired, averaging 64 (in ^2H_2O) or 128 (in ^1H_2O) transients of 2048 points, with 6024 Hz of spectral width. Time domain data matrices were all zero-filled in the ω_1 dimension to 2K, and to 4K in ω_2, thus yielding a digital resolution of 5.88 and 2.94 Hz/point, respectively. A 10°-shifted squared sine-bell in ω_2 and a Lorentz-Gauss resolution enhancement in ω_1 were used as window functions before transformation. Pure absorption NOESY spectra were obtained with different mixing times (60, 120, and 200 ms) with a 10% random variation of the mixing time to cancel scalar correlation effects (Macura et al., 1981). The MLEV-17 TOCSY experiments in ^1H_2O and ^2H_2O had mixing times of 36 and 68 ms, respectively.

Irradiation of the ^1H_2O resonance was achieved in the coherent mode (Zuiderweg et al., 1986), during the relaxation time, and, in the case of the NOESY, during the mixing time.

Slowly exchanging protons, at pH* 3.3 and 310 K, were identified by recording a NOESY spectrum of the hormone solution, freshly lyophilized from ^1H_2O, immediately after dissolution in ^2H_2O–SDS_{d25}. After a period of 24 h, nearly all of the amide protons were fully exchanged, but 20% of the resonances were still detectable.

Measurements of $^3J_{HN\alpha}$ coupling constants $\geq$7 Hz were obtained at 310 K from 1D experiments after zero filling to 128 K and application of strong Lorentz–Gauss resolution enhancement. Coupling constants $\leq$5 Hz could not be measured from 1D experiments because of the broadening brought about by SDS. They were estimated from the DQF-COSY spectrum so that they are reported as apparent values.

Estimation of Distance Restraints and Stereospecific Assignments. A semiquantitative correlation between NOESY cross-peak intensities and proton–proton distances was obtained by comparing the effects observed at different mixing times with the standard distances in protein structures (Wüthrich, 1986). Strong, medium, and weak intraresidual and sequential NOEs observed at 60 ms were translated into three distance ranges: 2.6–2.8, 2.9–3.1, and 3.3–3.6 Å, respectively. Looser upper limits were set for medium-range and long-range NOEs and for weak peaks observed only in the 120-ms and the 200-ms NOESY spectra, with cutoff distances of 4.0 and 4.5 Å, respectively. The interproton distance restraints comprised 99 intraresidue distances, 158 short- and medium-range interresidue distances relative to amino acids less than five positions apart in the sequence, and 3 long-range interresidue distances. Restraints on the Cys^1–Cys^7 disulfide bond and on hydrogen bonds were also imposed. For the disulfide bond, the S1γ–S7γ distance was constrained to a range of 1.9–2.1 Å, while the C1β–S7γ and C7β–S1γ distances were in the range of 2.5–3.5 Å (Williamson et al., 1985). Hydrogen-bond constaints were applied as upper bounds of 2.5 Å for the O–H distance and 3.5 Å for the N–O distance. They were explicitly included only when $d_{\alpha N}(i,i+3)$ and $d_{\alpha N}(i,i+4)$ NOES were both observed for a slow-exchanging amide proton, as evidence for the presence of hydrogen bonds in an α-helix (Wagner et al., 1987).

The β-methylene groups were stereospecifically assigned with the program HABAS (Güntert et al., 1989), which uses intraresidual and sequential NOEs and vicinal coupling constants $^3J_{HN\alpha}$ and $^3J_{\alpha\beta}$. A total of 12 β-methylene groups (namely, those of residues 5, 9, 11, 12, 13, 14, 15, 17, 18, 19, 20, and 22) out of 23 were stereospecifically assigned. For Gly^{10}, the procedure suggested by Esposito et al. (1987) was used. The validity of stereospecific assignments was counterchecked by evaluating their consistency with the DG structures. When no stereospecific assignment was possible for methyl and methylene protons, distance constraints were corrected for pseudoatom representation (Wüthrich et al., 1983). For methyl groups, an additional correction of 0.5 Å was added to take into account the multiplicity.

Calculations. DG calculations were performed with the DIANA program (Güntert et al., 1991). The variable target function was changed according to the standard strategy from level 1 to 32. A total of 40 starting structures were generated from random choices of dihedral angles. The best 13 structures, in terms of distance violations, were chosen for further refinement. EM calculations were performed with the GROMOS software package (van Gunsteren & Berendsen, 1987). In order to release the strain caused by bad van der Waal contacts, while retaining the features of the original DG structures, 200 steps of steepest descent REM followed by 200 steps of conjugate gradient REM were applied. After the first minimization, bond length constraints were applied with the SHAKE method (van Gunsteren & Berendsen, 1977; Ryckaert et al., 1977). The list of nonbonded neighboring atom pairs was updated every 10 cycles of the EM. A cutoff radius of 0.8 nm was used beyond which no nonbonded interactions were evaluated. Distance restraints obtained from NMR measurements were incorporated in the calculations as a semiharmonic potential function with a force constant of 500 kJ nm^{-2} mol^{-1}.

Graphical representation and RMSD analysis between structure pairs were carried out with the interactive graphic program WHATIF (Vriend, 1990) running on an Evans and Sutherland PS390 graphics system.

All calculations were carried out on the Local Area Vax Cluster of the European Molecular Biology Laboratory at Heidelberg, Germany.

Results

^1H NMR Assignments. The increased viscosity brought about by SDS_{d25} [η = 9.1 cP at 310 K, as measured for an equimolar (0.90 M) solution of SDS] broadens all resonances, especially the solvent line. This requires a careful power setting for ^1H_2O suppression to avoid spillover of the power and base-plane distortions in 2D experiments.

Identification of complete spin systems of all 32 residues was based on DQF-COSY and TOCSY and was complemented with NOESY when ambiguities arose. All the experiments were run at pH 3.7 and at the physiological pH 7.4, in order to separate overlapping resonances and check for

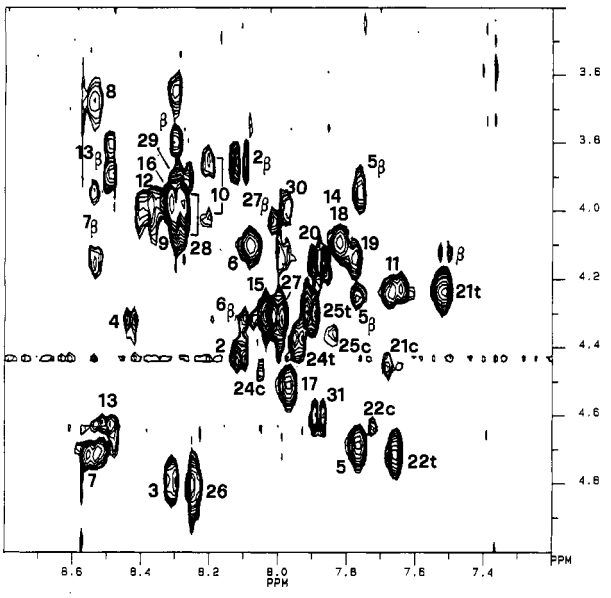

FIGURE 1: 500-MHz fingerprint region of a TOCSY spectrum (36-ms mixing time) of SDS_{d25}-bound sCT in 95% ^1H_2O/5% ^2H_2O, pH 3.7, 310 K. Connectivities are all labeled with the sequence number. For residues 21, 22, 24, and 25, a c (cis) or a t (trans) marks the minor and major form, respectively, due to cis–trans isomerism about the peptide bond of Pro^{23}.

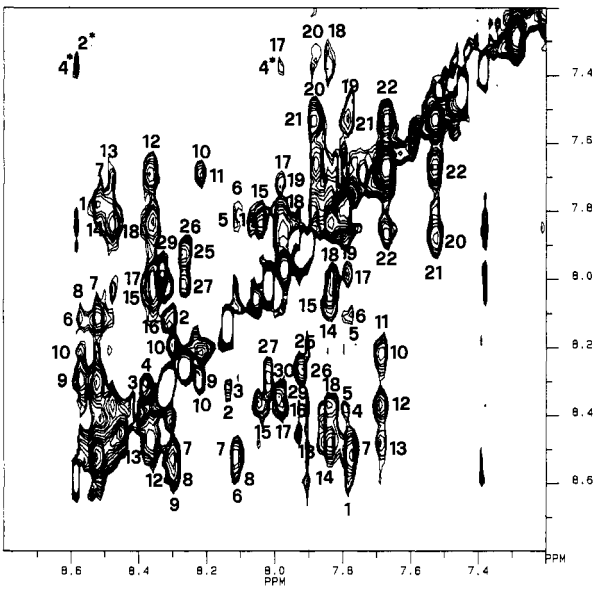

FIGURE 2: Amide region of a 200-ms mixing-time NOESY spectrum of SDS_{d25}-bound sCT in 95% ^1H_2O/5% ^2H_2O, pH 3.7, 310 K. Where space permits, connectivities are labeled with the sequence number. Asterisks mark NOEs involving the C(2)H and C(4)H of the His^{27} ring. For residues 21, 22, 24, and 25, only the major (trans) form is labeled because the minor (cis) form protons overlap with other signals.

possible conformational variations. A DQF-COSY and, in particular, a TOCSY spectrum with 36-ms mixing time, both in ^1H_2O, allowed the assignment of the $d_{N\alpha}$ connectivities (Figure 1). From the amide protons, relayed TOCSY connectivities assigned the aromatic spin systems (His^{17} and Phe^{22}) and the β protons of almost all of the amino acids. This allowed identification of the short side-chain residues (Gly, Ser, and Ala) but not of the long side-chain ones (Arg, Gln, Glu, Leu, Lys, and Pro). Their complete assignment was accomplished in ^2H_2O by a combination of DQF-COSY, 66-ms mixing-time TOCSY, and 200-ms mixing-time NOESY experiments. For example, the long-range connectivities between the ϵ protons of lysines and their α protons observed in the ^2H_2O TOCSY spectrum were very useful in linking the side chains of these residues to the NH_i–$C\alpha H_i$ fragment. The assignments of the Leu side chains were only possible through NOESY cross-peaks. In fact a comparison of the NH–aliphatic regions showed continuous intrachain cross-peaks in the NOESY but not in the TOCSY spectrum. The two Pro residues were also identified by typical NOE patterns. Strong connectivities were observed between the δ protons of one Pro and the NH proton of the unique Tyr^{22}, and to the NH proton of the unique Arg^{24}, thus identifying Pro^{23}. Cross-peaks from the other Pro Hδ protons to the Hα and the Hβ protons of a Thr (later identified as Thr^{31}) assigned Pro^{32}.

Evidence was found for the presence of an isomer with cis peptide bond for Pro^{23}, and it was estimated from the 1D spectrum to be about 20%. Its presence was revealed by a small NOE between the Hα protons of Tyr^{22} and Pro^{23}, while the trans form was identified by an effect between Tyr^{22} NH and the δ protons of Pro^{23}. This finding justifies the presence of seven Thr spin systems, whereas the primary sequence contains only five Thr residues (Scheme I). As previously reported for sCT in cryosolvent (Motta et al., 1989), conformational heterogeneity due to the relatively slow isomerization of cis and trans form of Pro^{23} brings about additional spin systems for nearby residues. Identical results have been reported for sCT in MeOH (Meadows et al., 1991), as well as for hCT (Motta et al., 1991). Resonances sensitive to the geometry of the Pro^{23} peptide bond are those of Thr^{21}, Tyr^{22}, Arg^{24}, and Thr^{25}. Their protons give separate signals for the cis and trans forms (labeled c and t, respectively) in the TOCSY fingerprint region (Figure 1). Pro^{32} was found to be predominantly in the trans configuration since only the effect between Thr^{31} and the Hδ protons of Pro^{32} was visible.

Sequential assignment information was obtained from Overhauser effects detected at 60-, 120-, and 200-ms mixing times. Figure 2 reports the NH–NH region of a NOESY spectrum at 200-ms mixing time. It is possible to follow the connectivities along virtually the entire length of the molecule, with only few interruptions. A particularly useful starting point for the sequential assignment was the unique amino acid spin system of Tyr^{22}. From its NH proton down to the Thr^6 NH, strong connections were seen clearly. Weaker effects were observed in the Cys^1–Ser^5 segment. Amide protons of Cys^1 were identified by a connectivity with the Cys^7 NH. At Pro^{23}, the loss of NH–NH connectivities was inevitable, but connectivities from Tyr^{22} NH to Pro^{23} Hδ and from Pro^{23} Hδ to Arg^{24} NH were seen in the fingerprint region of the NOESY spectrum. Connectivity between Arg^{24} and Thr^{25} was lost because of their degeneracy. However, except for the overlapping Gly^{28} and Ser^{29}, from Thr^{25} the NH–NH connectivities extend as far as Gly^{30}. The remaining two residues were identified by NOESY cross-peaks from the Pro^{32} δ protons to the Hα and the Hβ protons of preceding Thr. Complete assignments for sCT protons are given in Table I.

Secondary Structure. The secondary structure of sCT in SDS micelles was delineated from qualitative analysis of the sequential ($d_{\alpha N}$ and d_{NN}) and medium-range [$d_{\alpha N}(i,i+n)$, $n \geq 2$, and $d_{\alpha\beta}(i,i+3)$] NOES (Wüthrich, 1986), from slowly exchanging amide protons (Wüthrich, 1986), and from $^3J_{HN\alpha}$ coupling constants (Pardi et al., 1984) (Figure 3). The predominant structural feature is an α-helix. Positive evidence for helical structure (Wüthrich, 1986), i.e., absence of strong $d_{\alpha N}$ NOEs and the presence of d_{NN}, $d_{\alpha N}(i,i+3)$, and $d_{\alpha\beta}(i,i+3)$, is seen for the region Thr^6–Phe^{22}. Corroborative data for a helix come from slowly exchanging amides (except for Leu^{19} and Thr^{21}) and $^3J_{HN\alpha}$ coupling-constant values ≤ 5 Hz in that

Table I: Assignments of Proton Resonances of sCT in Aqueous SDS_{d25}, pH 3.7, at 310 K[a]

residue	shift of proton resonance (ppm) NH	αH	βH	others
Cys[1]	7.77	4.31	3.96, 3.71	
Ser[2]	8.13	4.43	3.98, 3.84	
Asn[3]	8.33	4.80	2.89, 2.79	δNH_2 7.45, 6.85
Leu[4]	8.41	4.32	1.73, 1.68	γCH 1.62; δCH_3 0.85, 0.80
Ser[5]	7.78	4.61	4.23, 3.95	
Thr[6]	8.09	4.10	4.32	γCH_3 1.35
Cys[7]	8.51	4.70	4.16, 3.93	
Val[8]	8.58	3.66	2.22	γCH_3 1.05, 0.89
Leu[9]	8.28	4.09	1.88, 1.85	γCH 1.60; δCH_3 1.04, 0.91
Gly[10]	8.22	4.04, 3.87		
Lys[11]	7.68	4.25	2.04, 1.93	γCH_2 1.60, 1.48; δCH_2 1.76, 1.76; ϵCH_2 2.94, 2.94; ϵNH_2 7.24
Leu[12]	8.37	3.99	1.86, 1.80	γCH 1.61; δCH_3 0.85, 0.81
Ser[13]	8.48	4.61	3.93, 3.81	
Gln[14]	7.82	4.10	2.32, 2.25	γCH_2 2.59, 2.42; δNH_2 7.21, 6.67
Glu[15]	8.05	4.29	2.02, 1.92	γCH_2 2.32, 2.15
Leu[16]	8.32	4.02	1.73, 1.62	γCH 1.58; δCH_3 0.85, 0.85
His[17]	7.97	4.52	3.38, 3.27	C(2)H 8.58; C(4)H 7.39
Lys[18]	7.82	4.10	2.01, 1.88	γCH_2 1.43, 1.43; δCH_2 1.74, 1.63; ϵCH_2 2.96, 2.96; ϵNH_2 7.16
Leu[19]	7.79	4.14	1.87, 1.63	γCH 1.52; δCH_3 0.93, 0.85
Gln[20]	7.87	4.16	2.17, 2.12	γCH_2 2.48, 2.39; δNH_2 6.80, 6.42
Thr[21]	7.53t	4.24t	4.15t	γCH_3 1.09t
	7.68c	4.46c	4.06c	γCH_3 1.25c
Tyr[22]	7.67t	4.73t	3.07t, 3.02t	C(2,6) 7.11t; C(3,5) 6.78t
	7.76c	4.66c	3.19c, 3.04c	C(2,6) 7.01c; C(3,5) 6.78c
Pro[23]		4.41	2.18, 1.71	γCH_2 1.91, 1.91; δCH_2 3.73, 3.33
Arg[24]	7.93t	4.38t	1.92t, 1.81t	γCH_2 1.75t, 1.62t; δCH_2 3.27t, 3.21t; ϵNH 6.67, 6.52
	8.04c	4.49c	1.92c, 1.86c	γCH_2 1.73c, 1.59c; δCH_2 3.31c, 3.19c
Thr[25]	7.91t	4.29t	4.28t	γCH_3 1.18t
	7.82c	4.37c	4.28c	γCH_3 1.22c
Asn[26]	8.26	4.82	2.83, 2.78	δNH_2 7.47, 6.78
Thr[27]	8.02	4.31	4.06	γCH_3 1.19
Gly[28]	8.31	4.08, 3.96		
Ser[29]	8.32	3.90	3.83, 3.64	
Gly[30]	7.98	4.09, 4.01		
Thr[31]	7.89	4.64	4.15	γCH_3 1.21
Pro[32]		4.37	1.98, 1.89	γCH_2 2.29, 2.29; δCH_2 3.80, 3.68

[a] c and t refer to cis and trans, respectively.

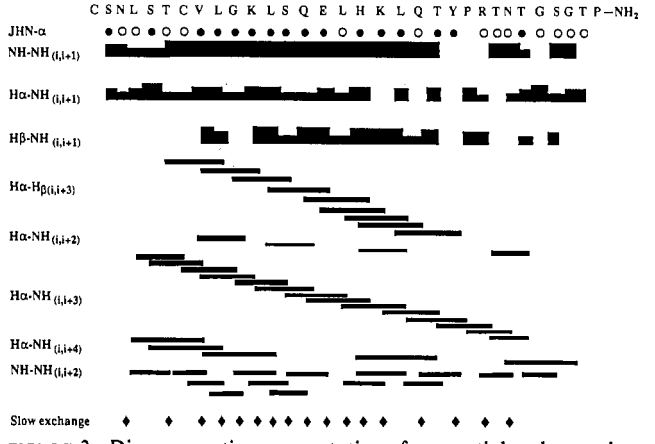

FIGURE 3: Diagrammatic representation of sequential and secondary structural interresidue NOEs observed for sCT in aqueous SDS_{d25}. NOE intensities are indicated by the height of the bars. Effects to the Hδ protons of Pro[23] and Pro[32], though observed, are not drawn. Circles indicate coupling constants data (●, apparent $^3J_{HN\alpha} \leq 5$; ○, measured $^3J_{HN\alpha} \geq 7$), while diamonds (♦) label residues for which slow exchange of NH protons with deuterons was observed.

region (Pardi et al., 1984). Here slow exchange is taken to indicate hydrogen bonding, since it is unlikely that a slowly exchanging proton is buried in the interior of a biomolecule as small as sCT.

Several intraresidual and sequential NOEs are observed for the Cys[1]–Cys[7] ring. However, characteristic medium-range NOEs (Thr[6] α–Leu[9]β and Cys[7] α–Gly[10] NH), present at all mixing times, indicate that Thr[6] and Cys[7] are certainly part of the helix. Also Leu[4] and Ser[5] show medium-range NOEs $d_{\alpha N}(i,i+3)$, at all mixing times, and $d_{\alpha N}(i,i+4)$, at a 200-ms mixing time only. This suggests that the helix termination may actually include also residues 4 and 5.

For the C-terminal decapeptide Pro[23]–Pro[32], we essentially found sequential NOEs. However, a few medium- and long-range NOEs were also observed (Figure 3). Some recall those expected for turns (Wagner et al., 1986), but some connect residues far apart in the sequence: Thr[31] NH–His[17] $CH_2\beta$, Asn[26] NH–Lys[18] $CH_2\delta$, and Asn[26] NH–Leu[19] CHγ. These NOEs indicate that the last 10 C-terminal residues form a loop folded toward the helix.

It is well known that helix formation under the influence of SDS is enhanced by a decrease in pH (Su & Jirgensons, 1977); however, examination of the NOE patterns at pH 7.4 (not shown) indicates that this structure is preserved at physiological pH.

Three-Dimensional Structure. Three-dimensional structures of sCT were generated consistently with the NMR data by combined use of DG and restrained energy minimization. From the initial structures generated by DG, 13 were selected for further refinement. They had no violations of the upper and lower bounds of the NMR distance restraints greater than 1.2 Å and did not predict any additional short interproton distance with no observable NOEs. The energy of these refined structures were all in the narrow range from −1364 to −1701 kJ mol^{-1}. The overall agreement among the 13 individual conformers can be seen by global RMSD comparisons. Table II lists the RMSD of the backbone atoms and of all atoms for these structures after EM. The average RMSD of

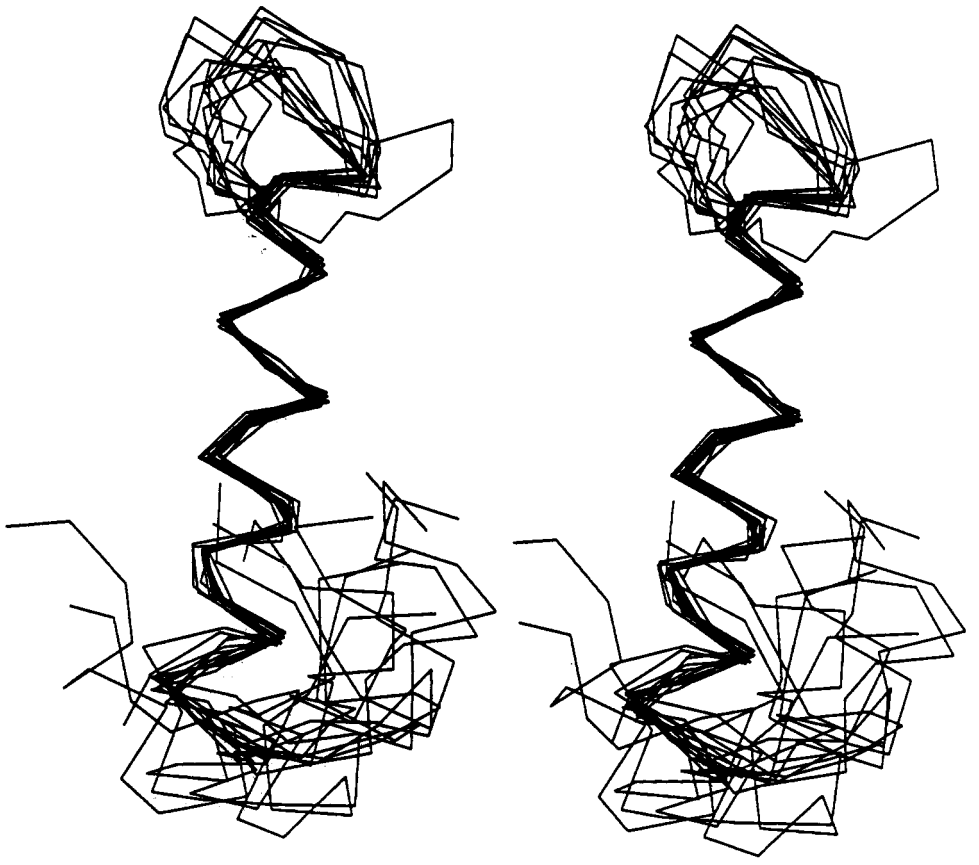

FIGURE 4: Stereoview of the Cα atoms of the 13 energy-refined DIANA structures of SDS_{d25}-bound sCT. Structures were superimposed for pairwise minimum RMSD of the Cα atoms of residues 6–22 with the lowest energy structure.

Table II: Comparison between Structure Pairs after Energy Minimization: Averaged RMSD (Å)[a]

	backbone	side chains	all atoms
all residues	3.59 (1.06)	5.50 (1.73)	4.58 (1.39)
residues 6–22	0.93 (0.35)	2.85 (0.66)	2.13 (0.50)

[a] The standard deviations are indicated in parentheses.

the backbone atoms is 3.59 Å, and this value is reduced to 0.93 Å when the better defined region comprising residues 6–22 is considered. The average distance restraint violation for these structures is 0.06 Å.

Figure 4 shows a superposition for the polypeptide backbone of the 13 structures obtained with the program DIANA and locally improved with REM. A unique backbone fold is obtained for residues 6–22, in which only Cys^7 and Leu^{16} were not stereospecifically assigned. Lack of convergence is instead observed in the C-terminal Pro^{23}–Pro^{32} decapeptide and, to a lesser degree, in the N-terminal part of the disulfide-bridged loop. The effect of energy minimization was to regularize the structures and to reduce the spread of the backbone dihedral angles. The distribution of ϕ and ψ angles (Figure 5) of the six lowest energy structures reflects the extent to which the conformation has been defined by NOE constraints. Good agreement was observed among the structures for the values of ϕ and ψ of the helical region (Thr^6–Tyr^{22}). Residues Cys^1–Ser^5 (Figure 5A,B) do not converge to a unique structure, even though Leu^4 presents values expected for a helix. However, the spreading observed for Ser^5 angles does not allow inclusion of residues 4 and 5 into the helix. From Pro^{23} onward, the lack of convergence reflects the absence of many structurally significant NOE restraints for the C-terminal decapeptide, even though some long-range NOEs (see above) limit the accessible conformational space.

Discussion

The spectrum of sCT in SDS micelles, used to simulate the interface, has been completely assigned by 2D NMR spectroscopy. Secondary structure identification relied upon the observed NOE patterns, $^3J_{HN\alpha}$ coupling constants, and amide proton exchange data. NOESY cross-peaks observed in 60-, 120-, and 200-ms spectra were classified according to their intensity and employed as distance constraints for structure calculations with the DG program DIANA. Selected structures were subsequently energy refined with the GROMOS program. The predominant conformational feature of sCT in SDS_{d25} micelles is an amphipathic α-helix between residues 6 and 22 (Figure 4), which contains the segment 8–22 found in TFE (Meyer et al., 1991) and MeOH (Meadows et al., 1991). The inclusion of Thr^6 and Cys^7 into the helix is supported by the interresidual NOEs (Figure 3) and the backbone torsion angles (Figure 5). The ϕ and ψ values suggest that also Leu^4 is in the allowed α-helical region. However, the lack of convergence among the structures for Ser^5 (Figure 5) does not warrant the inclusion of residues 4 and 5 into the helix, thus keeping its N-termination at Thr^6. Nevertheless, as suggested by Meadows et al. (1991), residues Cys^1–Ser^5 may act to stabilize the N-terminus of the helix. Indeed Ser (found at sites 2 and 5) and Asn (found at site 3), together with Thr, have been shown to have good ability in stabilizing the N-terminus of an α-helix (Richardson & Richardson, 1990).

The Pro^{23}–Pro^{32} region is found in close association with the helix. The short- and medium-range NOEs observed (Figure 3), indicate the presence of a hinge involving residues 22–25, which favors the formation of a loop and justifies the observed long-range contacts (Thr^{31} NH–His^{17} $CH_2\beta$, Asn^{26} NH–Lys^{18} $CH_2\delta$, and Asn^{26} NH–Leu^{19} CHγ). A loop of a shorter length (Meyer et al., 1991) was found in TFE but not

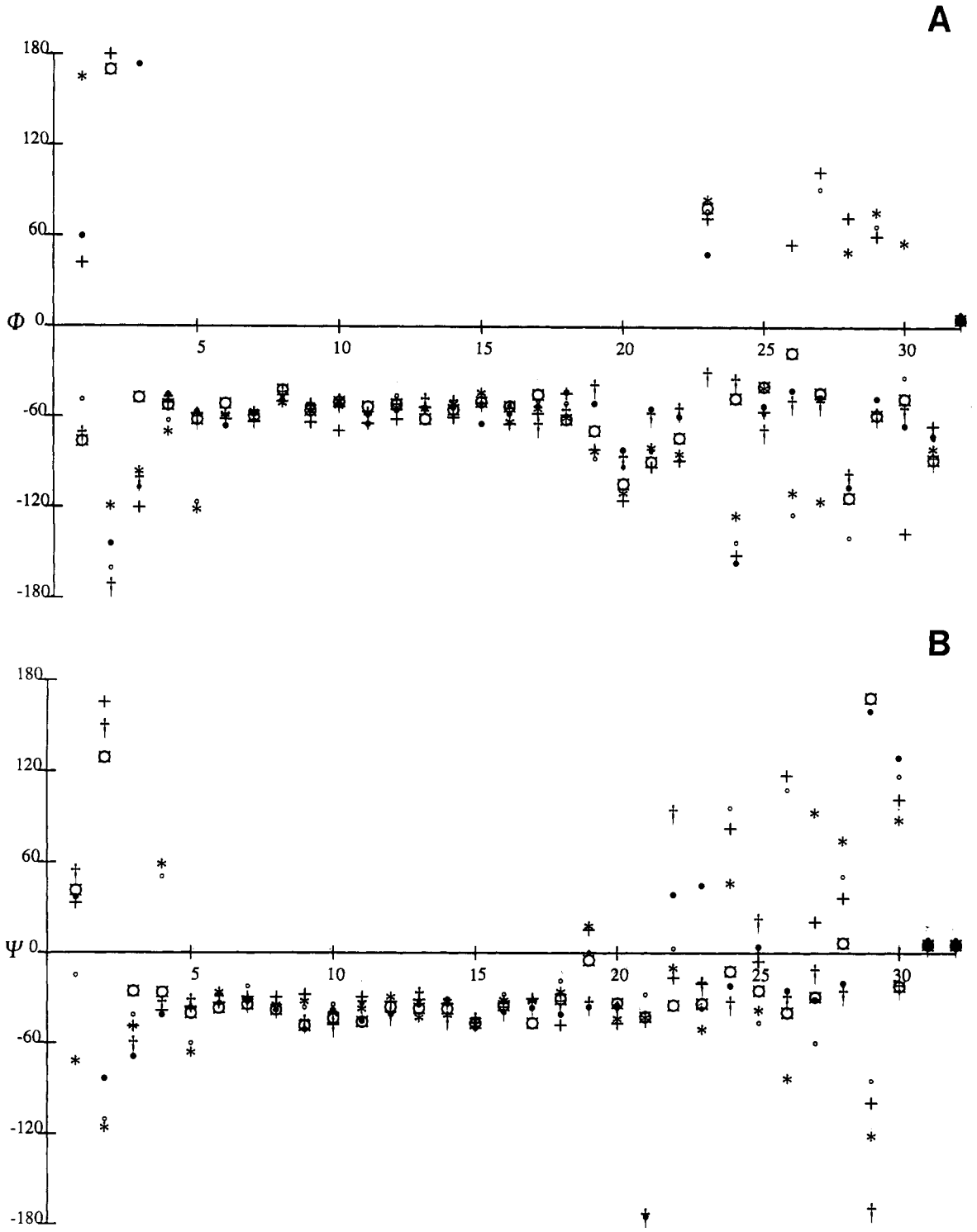

FIGURE 5: Comparison of the ϕ angles (A) and ψ angles (B) for each residue in six representative energy-refined structures.

in MeOH, in which the C-terminal segment was found to exist in an extended conformation with no interaction with the helix (Meadows et al., 1991).

The ability of sCT and human calcitonin gene-related peptide (hCGRP) to cross-react at their respective receptors is taken as an indication that some secondary structural elements are shared by both hormones (Breimer et al., 1988, and references therein). The solution structure of hCGRP in a TFE–water mixture (Breeze et al., 1991) consists of a well-defined N-terminal disulfide-bonded loop (residues 2–7) followed by an α-helix (residues 8–18); thereafter, the structure is predominantly disordered with a poorly defined turn-type conformation between residues 19 and 21. Accordingly, structural similarities between hCGRP and sCT are observed in the N-terminal and helix regions but not in the C-terminal region, which folds back toward the helix in our sCT structure.

It has been proposed that long-range interactions affect receptor binding and/or conformational properties of the receptor-bound hormone. In particular, interactions between the amino- and the carboxyl-terminal regions of the molecule, thought to be juxtaposed in spatial configuration (Byfield et al., 1972), have been invoked to interpret different activities between the hormone and its derivatives (Epand et al., 1986a). The structure of SDS_{d25}-bound sCT shows no interaction

between the N- and C-termini but between the helix and the C-terminus. The properties of amphipathic polypeptides at the interfaces indicate that the amphipathic structural element is likely to be induced on cell surfaces (Taylor & Ösapay, 1990). In fact, the types of interactions that may be operative in the SDS micellar system recall those important for protein–lipid association in membrane (Gierash et al., 1982). Therefore, at the surface simulated by SDS, a cooperative conformational interaction between the α-helix and the C-terminus takes place. This finding seems to be in agreement with loss of biological activity brought about by shortening of the C-terminal end (Epand et al., 1986b) and with the full retention of the biological activity in salmon calcitonins modified at the N-terminal residues (Breimer et al., 1988, and references therein).

Further investigations to better assess the role of this interaction are in progress.

ACKNOWLEDGMENTS

We thank Dr. Lucia Zetta (CNR, Milano, Italy) for instrument time on her 500-MHz spectrometer, Dr. Henriette Molinari (Università di Milano, Italy) for technical advice, Dr. Gerrit Vriend (EMBL, Heidelberg, Germany) for his kind assistance in the use of the WHATIF program, Dr. Vladimir Saudek and co-workers (Merell Dow Research, Strasbourg, France) for sending us their manuscript prior to publication, Dr. Donato Ciccarelli (Università di Napoli, Italy) for measuring the viscosity of the SDS solution, and Prof. A. M. Lesk for his warm hospitality to M.A.C.M.

Registry No. CT, 9007-12-9; SDS, 151-21-3.

REFERENCES

Bax, A., & Davis, D. (1985) *J. Magn. Reson. 65*, 355–366.
Braunschweiler, L., & Ernst, R. R. (1983) *J. Magn. Reson. 53*, 521–528.
Breeze, A. L., Harvey, T. S., Bazzo, R., & Campbell, I. D. (1991) *Biochemistry 30*, 575–582.
Breimer, L. H., MacIntyre, I., & Zaidi, M. (1988) *Biochem. J. 255*, 377–390.
Byfield, P. G. H., Clarke, M. B., Turner, K., Foster, G. V., & MacIntyre, I. (1972) *Biochem. J. 127*, 199–206.
Dayhoff, M. O. (1978) *Atlas of Protein Sequence and Structure*, National Biomedical Research Foundation, Silver Spring, MD.
Doi, M., Yamanaka, Y., Kobayashi, Y., Kyogoku, Y., Takimoto, M., & Gota, K. (1989) *Structure Study of Human Calcitonin, Proc. Am. Pept. Symp., 11th* (Rivier, J. E., & Marshall, G. R., Eds.) LaJolla, CA.
Drobny, G., Pines, A., Sinton, S., Weitkamp, D., & Wemmer, D. (1979) *Faraday Symp. Chem. Soc. 13*, 49–55.
Epand, R. M. (1983) *Mol. Cell. Biochem. 57*, 41–47.
Epand, R. M., Epand, R. F., Orlowski, R. C., Schlueter, R. J., Boni, L. T., & Hui, S. W. (1983) *Biochemistry 22*, 5074–5084.
Epand, R. M., Epand, R. F., & Orlowski, R. C. (1985) *Int. J. Pept. Protein Res. 25*, 105–111.
Epand, R. M., Epand, R. F., Orlowski, R. C., Seyler, J. K., & Colescott, R. L. (1986a) *Biochemistry 25*, 1964–1968.
Epand, R. M., Stahl, G. L., & Orlowski, R. C. (1986b) *Int. J. Pept. Protein Res. 27*, 501–506.
Esposito, G., Carver, J. A., Boyd, J., & Campbell, I. D. (1987) *Biochemistry 26*, 1043–1050.
Gierasch, L. M., Lacy, J. E., Thompson, K. F., Rockwell, A. L., & Watnick, P. I. (1982) *Biophys. J. 37*, 275–284.
Güntert, P., Braun, W., Billeter, M., & Wüthrich, K. (1989) *J. Am. Chem. Soc. 111*, 3997–4004.
Güntert, P., Braun, W., & Wüthrich, K. (1991) *J. Mol. Biol. 217*, 517–530.
Macura, S., & Ernst, R. R. (1980) *Mol. Phys. 41*, 95–117.
Macura, S., Huang, Y., Suter, D., & Ernst, R. R. (1980) *J. Magn. Reson. 43*, 259–281.
Meadows, R. P., Nikonowicz, E. P., Jones, C. R., Bastian, J. W., & Gorenstein, D. G. (1991) *Biochemistry 30*, 1247–1254.
Merle, M., Lefevre, G., & Milhaud, G. (1979) *Biochem. Biophys. Res. Commun. 87*, 455–460.
Meyer, J.-P., Pelton, J. T., Hoflack, J., & Saudek, V. (1991) *Biopolymers 31*, 233–241.
Motta, A., Picone, D., Tancredi, T., & Temussi, P. A. (1987) *J. Magn. Reson. 75*, 364–370.
Motta, A., Picone, D., Tancredi, T., & Temussi, P. A. (1988) *Tetrahedron 44*, 975–990.
Motta, A., Castiglione-Morelli, M. A., Goud, N., & Temussi, P. A. (1989) *Biochemistry 28*, 7998–8002.
Motta, A., Temussi, P. A., Wünsch, E., & Bovermann, G. (1991) *Biochemistry 30*, 2364–2371.
Pardi, A., Billeter, M., & Wüthrich, K. (1984) *J. Mol. Biol. 180*, 741–751.
Piantini, U., Sørensen, O. W., & Ernst, R. R. (1982) *J. Am. Chem. Soc. 104*, 6800–6801.
Richardson, J. S., & Richardson, D. C. (1990) in *Prediction of Protein Structure and the Principles of Protein Conformation* (Fasman, G. D., Ed.) pp 1–98, Plenum Publishing Corp., New York.
Ryckaert, J. P., Ciccotti, G., & Berendsen, H. J. C. (1977) *J. Comput. Phys. 23*, 327–341.
Segrest, J. P., De Loof, H., Dohlman, J. G., Brouillette, C. G., & Anantharamaiah, G. M. (1990) *Proteins 8*, 103–117.
Schwyzer, R. (1986) *Biochemistry 25*, 6335–6342.
Su, Y.-Y. T., & Jirgensons, B. (1977) *Arch. Biochem. Biophys. 181*, 137–146.
Taylor, J. W., & Ösapay, G. (1990) *Acc. Chem. Res. 23*, 338–344.
van Gunsteren, W. F., & Berendsen, H. J. C. (1977) *Mol. Phys. 34*, 1311–1327.
van Gunsteren, W. F., & Berendson, H. J. C. (1987) *Groningen Molecular Simulation* (GROMOS) *Library Manual*, pp 1–229, BIOMOS, Groningen, The Netherlands.
Vriend, G. (1990) *J. Mol. Graphics 8*, 52–56.
Wagner, G., Neuhaus, D. Wörgötter, E., Vasak, M., Käji, J. R. H., & Wüthrich, K. (1986) *J. Mol. Biol. 187*, 131–135.
Wagner, G., Braun, W., Havel, T. F., Schaumann, T., Go, N., & Wüthrich, K. (1987) *J. Mol. Biol. 196*, 611–639.
Williamson, M. P., Havel, T. F., & Wüthrich (1985) *J. Mol. Biol. 182*, 295–315.
Wüthrich, K. (1986) *NMR of Proteins and Nucleic Acids*, J. Wiley & Sons, New York.
Wüthrich, K., Billeter, M., & Braun, W. (1983) *J. Mol. Biol. 169*, 949–961.
Zuiderweg, E. R. P., Hallenga, K., & Olejniczak, E. T. (1986) *J. Magn. Reson. 70*, 336–343.